Geometric Modeling of Epicycloid Hypoid Gear Based on Processing Principle

He Ying[1], He Guo Qi[2], Yan Hong Zhi[3], Liu Ming[4]

[1]Department of Resources Engineering Hunan Vocational Institute of Technology, Xiangtan 411104 China

[2]School of Mechanical Engineering Hunan University of Technology, Zhuzhou 412007 China

[3, 4]College of Mechanical and Electrical Engineering, Central South University, Changsha 410083 China

[1]503904249@qq.com; [2]1045894824@qq.com; [3]tjhgq@163.com; [4]937651483@qq.com

***Abstract*-According to the processing principles of gear cutting, tool structure, and the relevant position and movement between the machine and the work piece, this study established the optimal meshing coordinate for gear cutting by using the gear cutting meshing principle. Nonlinear equations were established by data discrimination of theoretical tooth surfaces; they were solved by MATLAB software, and three-dimensional coordinates of disperse points on the tooth surface are obtained. Three-dimensional coordinates were introduced into Pro/E software, and a three-dimensional geometry model of cycloid hypoid gear was built. Finally, dynamic simulation of the cycloid hypoid gear was performed, verifying the accuracy of the 3D model.**

Keywords- Cycloid Tooth; Hypoid Gear; Tooth Surface Equation; Geometric Modelling

I. INTRODUCTION

Spiral bevel gear is a key component of many mechanical products, such as the automobile, machine tools and aviation equipments [1-6]. Hypoid gear is generally divided into arc gear, cycloid gear and quasi involutes tooth systems. The processing method of continuous indexing has greatly improved the production efficiency of cycloid gear, making it a popular topic of current research [8-10]. Many domestic and foreign scholars have conducted research on cycloid, most of which provide analysis of the two meshing tooth, while the actual modeling process has not been clarified in detail or strictly verified [3-9]. There are some remaining problems in cycloid gear research such as its complicated understanding and unclear parameters, and the lack of consideration to the geometry of the cutter head and other elements. Particularly, when cycloid gear is produced by the machine tool PHOENIX® II 600HC, the cutter head revolves around the wobble platform, so the cycloid bevel gear is more complicated than the spiral bevel gear often used in theoretical and geometric modeling.

Because the shape of the tooth surface of epicycloid hypoid gear is complex and directly affected by the machining parameters, it is difficult to use CAD software to make precise models based on direct observation. This paper studies the cycloid tooth produced by the PHOENIX® II 600HC, and primarily analyzes the derivation of tooth surface equations and geometric modeling, to provide a model foundation for the study of cycloid hypoid gear [9-13].

II. MESHING THEORY OF HYPOID GEAR DRIVE

The formation of dividing a conical surface for hypoid gear pairing is shown in Fig. 1. The most favorable reference point M is randomly chose, and the only straight line is made through point M, respectively intersecting two gear axes at K_1 and K_2. A dividing plane T is made perpendicular to $\overline{K_1K_2}$ and through point M, so that plane T intersects two gear axes at O_1' and O_2'. A pair of dividing conical surfaces tangent to point M are formed by the respective revolutions of generatrixes $\overline{O_1'M}$ and $\overline{O_2'M}$ around two gear axes; they are separately tangent to plane T in the direction of lines $\overline{O_1'M}$ and $\overline{O_2'M}$. The distance r_{m1} and r_{m2} from point M to two gear axes are the radii of two gear pitches. The two angles δ_1 and δ_2 between the dividing cone generatrixes $\overline{O_1'M}$ & $\overline{O_2'M}$ and the two respective gear axes are the dividing cone angles of the two gears.

DOI: 10.5963/IJEE0503003

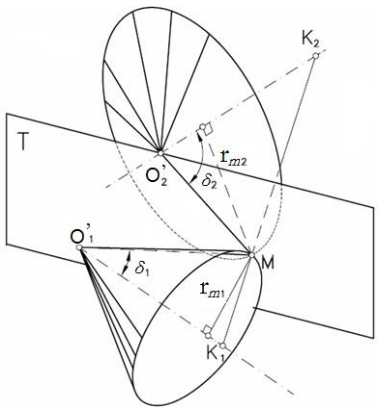

Fig. 1 Formation of dividing conical surface for hypoid gear pair

III. TOOTH SURFACE EQUATION OF HYPOID GEAR

A. *Relative Motion for Continuously Dividing Gear Mill*

As shown in Fig. 2, the cutter head contains z_0 groups of cutter teeth with r_0 as the nominal radius. The tooth number of gear billets is z_i; the tooth number of the generating gear is z_p. The cutter head rotates on its axle center O_0, while its axis revolves on the axle center O_p of the generating gear; the two rotation directions are the same. The relative motion between the cutter head and the generating gear can be recognized as pure rolling on the generating gear base circle with a radius of E_y, and the cutter head rolling circle with radius E_b. The distance from point O_0 to point O_p is described as the radial cutter location E_x, and is the known quantity of the machine tool adjustment card. ω_t, ω_i and ω_p respectively denote the angular velocity of the cutter head, wheel blank, and generating gear. The relative motion between the cutter head and gear billets satisfy continuous graduation, and it can be expressed by drive ratio R_b, as follows:

$$R_b = \frac{\omega_i}{\omega_t} = \frac{z_0}{z_i} \tag{1}$$

The cutter head and generating gear satisfy the following relations:

$$\frac{\omega_t}{\omega_p} = \frac{z_p}{z_0};\quad E_y = \frac{z_p}{z_0 + z_p} E_x;\quad E_b = \frac{z_0}{z_0 + z_p} E_x;\quad \frac{\omega_i}{\omega_p} = \frac{z_p}{z_i} = R_a \text{ (Rolling Ratio).}$$

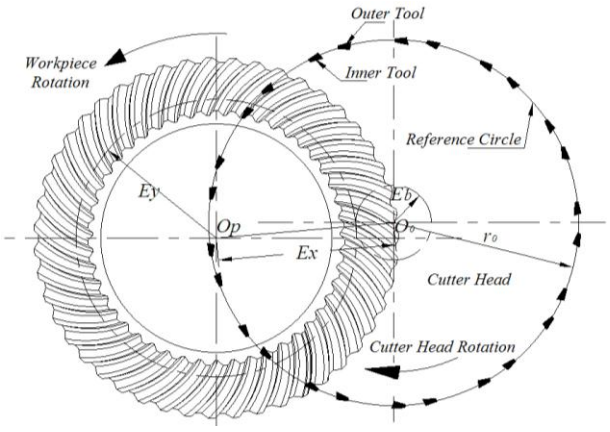

Fig. 2 Principle of cycloid formation

B. *Parameters of TRI-AC Cutter Head*

DOI: 10.5963/IJEE0503003

Fig. 3 depicts a TRI-AC cutting edge; r_t represents the arc radius of the cutting edge; α represents the pressure angle between axis Z_b and tangent of O_b; h_b represents the distance from the cutter node to the tool nose; u represents the distance from the cutter node P (O_b) to any point in the direction of cutting edge to cutter tip.

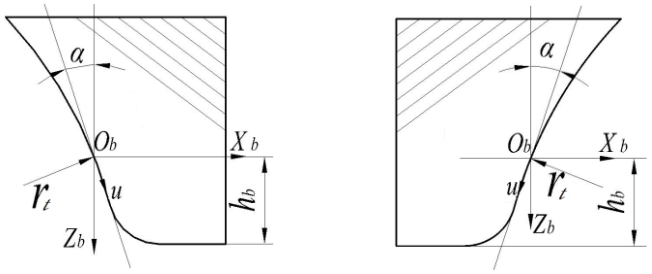

(a) Coordinate of inner cutting edge (b) Coordinate of outer cutting edge

Fig. 3 Cutting edge coordinates

Fig. 4 Cutter coordinates

As shown in Fig. 4, the coordinate system S_b is transformed into coordinate system S_c where η_c represents the anterior horn, usually set to 12 degrees; η_d represents the tilt angle of the blade installation of 4.42 degrees. Then the coordinate system S_c is transformed into coordinate system S_d; the corresponding transformation matrixes are $\boldsymbol{M}_{cb}$ and $\boldsymbol{M}_{dc}$.

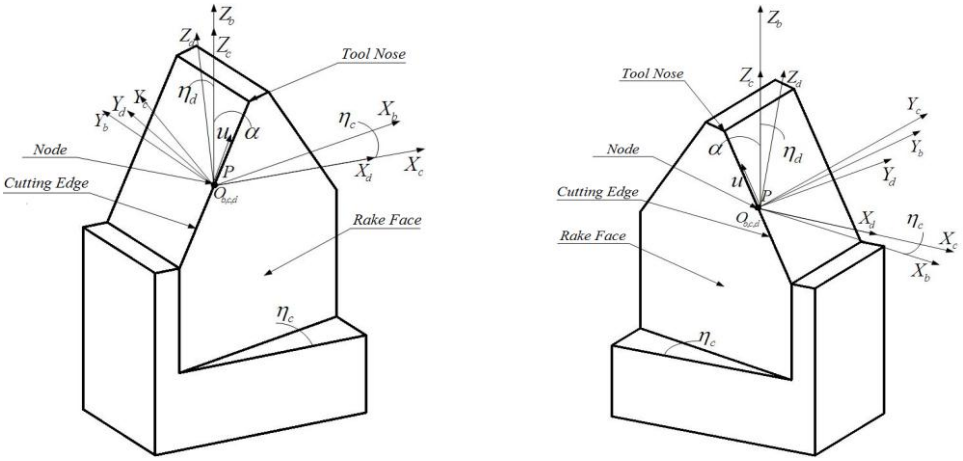

(a) Coordinate of inner cutter (b) Coordinate of outer cutter

As shown in Figs. 5 and 6, the plane XY is made through cutter node P, and is perpendicular to the axes of the cutter head. Cutter node P is the origin O_d of the coordinate system S_d, and coordinate system S_e revolves around the cutter head. The origins O_e and O_f are coincident. ε Represents the direction angle of the cutter tooth, and θ represents the rotation angle of the cutter head. Coordinate system S_d is successively transformed into coordinate systems S_e and S_f, and the corresponding transformation matrixes are $\boldsymbol{M}_{ed}$ and $\boldsymbol{M}_{fe}$. The mathematical expressions $\boldsymbol{r}_f(u,\theta)$ of the blade in the coordinate system S_f is finally drawn derived as in equation 7, and contains two parametric variables u and θ.

DOI: 10.5963/IJEE0503003

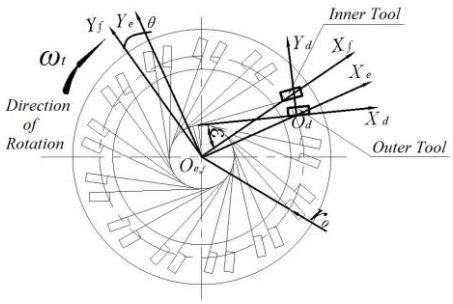

Fig. 5 TRI-AC cutter head processing left lateral pinion

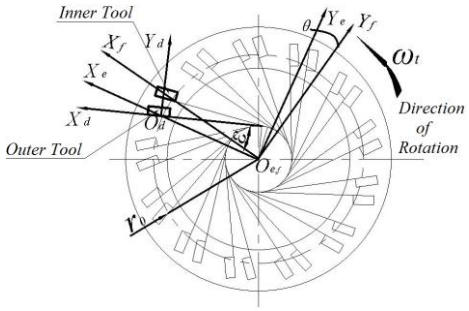

Fig. 6 TRI-AC cutter head processing right lateral large gear

IV. MOTION MODEL OF MACHINE TOOL

A motion model of all motor units and shaft systems for the PHOENIX®II 600HC bevel gear cutting machine is shown in Fig. 7. Motion 1 and 2 respectively denote the rotation of the cutter head and the work piece, and Motion 3 denotes adjustment for the installation angle of the wheel blank. X_b denotes the position of the machine tool. X_p and E_m respectively denote the location of the gear in the horizontal and vertical position.

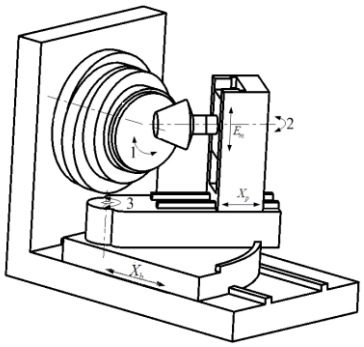

Fig. 7 Motion model of cycloid cutting machine

A. Transformation of Machine Tool with Evolutional Method of Machining

The tilting structure is shown in Fig. 8. The coordinate system S_f is transformed into coordinate system S_j, and the transformation matrix is $\boldsymbol{M}_{jf}$; i represents the tilting angle.

DOI: 10.5963/IJEE0503003

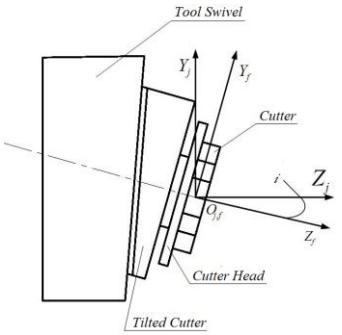

Fig. 8 Coordinate systems S_j and S_f

As shown in Fig. 9, coordinate system S_m generates motion with a wobble platform; coordinate system S_k is stationary relative to coordinate system S_m. q_0 represents the initial value of the cutter location in angular orientation; E_x represents the value of the radial cutter location; j represents the rotation angle of the tool. Coordinate system S_j is successively transformed into coordinate systems S_k and S_m, and the corresponding transformation matrixes are $\boldsymbol{M}_{kj}$ and $\boldsymbol{M}_{mk}$.

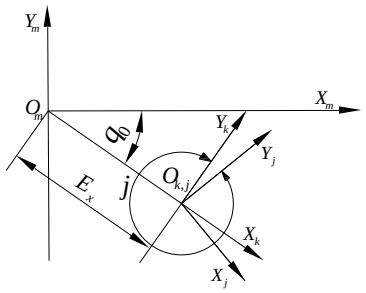

Fig. 9 Coordinate systems S_m, S_k and S_j

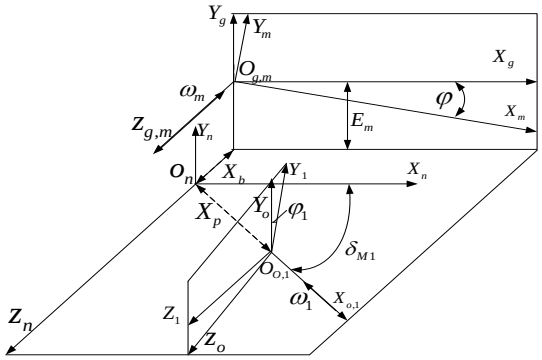

Fig. 10 All coordinates of machine tool with evolutional method of machining

As shown in Fig. 10, the coordinate system S_g of the machine tool is absolutely stationary. Coordinate systems S_m and S_g are initially coincident. Then, the wobble platform generatues motion with an angular velocity of ω_m, and parametric variable φ represents the rotational angle at any moment. δ_{M1} denotes the installation angle of the machine tool. The work piece rotates with an angular velocity of ω_1, and φ_1 represents its rotational angle at any moment. According to the continuous dividing generating theory, the equality, $\varphi_1 = R_b\theta + R_a\varphi$, is drawn.

B. Motion Transformation of Machine Tool with Shaping Method

As shown in Fig. 11, the coordinate system S_m is stationary, and consolidated to the machine tool. Coordinate system S_k rotates with the cutter head, and is consolidated to it. Coordinate systems S_l and S_o are stationary relative to coordinate system S_m. Coordinate system S_2 rotates with the work piece at the angular velocity of ω_m and φ_2 and represents its rotational angle at any moment. According to the continuous dividing generating theory, the equality, $\varphi_2 = R_b\theta$, is drawn. H_2

DOI: 10.5963/IJEE0503003

and V_2 respectively represent cutter location in the horizontal and vertical direction, and δ_{M2} represents the installation angle.

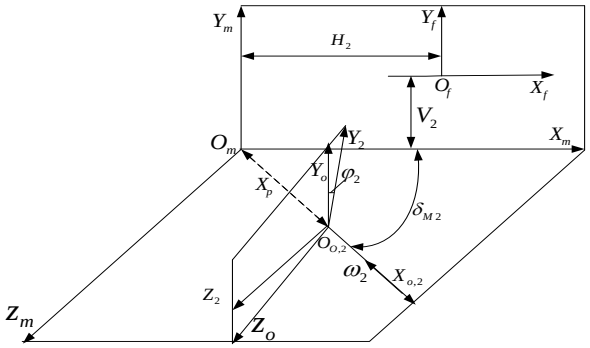

Fig. 11 All coordinates of machine tool with shaping method

V. GEOMETRIC MODELING OF HYPOID GEAR

A. Tooth Surface Equation

$\boldsymbol{r}_f(u,\theta)$ is respectively transformed into coordinate systems S_1 and S_2, and the tooth surface equations of pinion and large gear are obtained, as shown in equations 2 and 3. The surface obtained by means of this evolutional method of machining contains three unknown quantities: u, θ and φ, while the surface obtained by means of the shaping method contains two unknown quantities: u and θ.

$$\boldsymbol{r}_1(u,\theta,\varphi)=\boldsymbol{M}_{1o}(u,\theta)\cdot\boldsymbol{M}_{on}\cdot\boldsymbol{M}_{ng}\cdot\boldsymbol{M}_{gm}(\varphi)\cdot\boldsymbol{M}_{mk}\cdot\boldsymbol{M}_{kj}\cdot\boldsymbol{M}_{jf}\cdot\boldsymbol{r}_f(u,\theta) \tag{2}$$

$$\boldsymbol{r}_2(u,\theta)=\boldsymbol{M}_{2o}(\theta)\cdot\boldsymbol{M}_{om}\cdot\boldsymbol{M}_{mf}\cdot\boldsymbol{r}_f(u,\theta) \tag{3}$$

According to the gear meshing theory, a meshing equation can be obtained for an evolutional method of machining, that is as follows:

$$\boldsymbol{f}_1(u,\theta,\varphi)=\boldsymbol{n}_1\cdot\frac{\partial\boldsymbol{r}_1}{\partial\varphi}=0 \tag{4}$$

where $\boldsymbol{n}_1$ is the normal vector of tooth surface.

B. Calculation of Tooth Surfaces Points

The rotary projection is made through the gear axial section, which is shown in Fig. 12, and the grids scheme is accomplished on the tooth surface. In order to be easily understood and solved, it is first solved in the coordinate system $S_h(o_h,x_h,y_h)$. x_h represents generatrix dividing pyramid, and $o_{h,1}$ is conical vertex of gear billets.

$$\begin{cases}x_h=x, x\in[R_i,R_e]\\ y_h=y, y\in[-h_f,h_a]\end{cases} \tag{5}$$

In equations 5, R_i and R_e respectively represent the cone distance between the gear billet's small end and its big end; h_f and h_a respectively represent the height of the tooth root and addendum. Coordinate system S_h is transformed into coordinate system S_1, and we derive:

$$\boldsymbol{r}(x_1,y_1)=\boldsymbol{M}_{1h}\boldsymbol{r}(x_h,y_h) \tag{6}$$

where $\boldsymbol{M}_{1h}=\begin{bmatrix}\cos\delta & -\sin\delta\\ \sin\delta & \cos\delta\end{bmatrix}$, $\boldsymbol{r}(x_h,y_h)=[x,y]^T$, the x_1 axis and x_h are coincident.

DOI: 10.5963/IJEE0503003

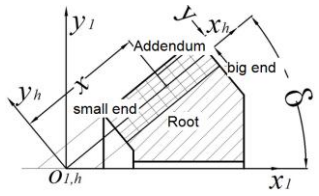

Fig. 12 Grids Schema on Tooth Surface

According to established tooth surfaces, the equations of tooth surface (equations 7 and 8) for a pinion and large gear are obtained by an evolutional method of machining.

$$\begin{cases} \boldsymbol{r}_1(u,\theta,\varphi) = \boldsymbol{M}_{1o}(u,\theta)\cdot\boldsymbol{M}_{on}\cdot\boldsymbol{M}_{ng}\cdot\boldsymbol{M}_{gm}(\varphi)\cdot\boldsymbol{M}_{mk}\cdot\boldsymbol{M}_{kj}\cdot\boldsymbol{M}_{jf}\cdot\boldsymbol{r}_f(u,\theta) \\ \boldsymbol{f}_1(u,\theta,\varphi) = \boldsymbol{n}_1\cdot\dfrac{\partial\boldsymbol{r}_1}{\partial\varphi} = 0 \\ \boldsymbol{r}(x_1,y_1) = \boldsymbol{M}_{1h}\cdot\boldsymbol{r}(x_h,y_h) \end{cases} \tag{7}$$

$$\begin{cases} \boldsymbol{r}_2(u,\theta) = \boldsymbol{M}_{2o}(\theta)\bullet\boldsymbol{M}_{om}\cdot\boldsymbol{M}_{mf}\cdot\boldsymbol{r}_f(u,\theta) \\ \boldsymbol{r}(x_1,y_1) = \boldsymbol{M}_{1h}\cdot\boldsymbol{r}(x_h,y_h) \end{cases} \tag{8}$$

Nonlinear equations are solved by discrimination of the tooth surface, thus obtaining the corresponding coordinate values. All coordinate values are solved by Matlab7.0 software. Part of the values is chosen, and a graph is drawn based on three-dimensional coordinate values, as shown in Fig. 13.

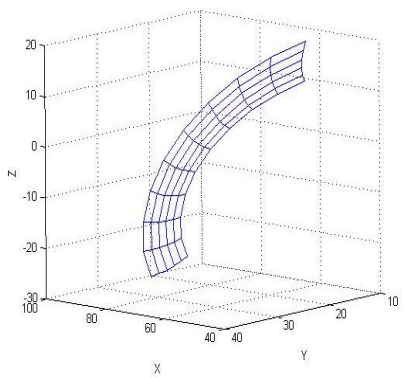

(a) Concave of pinion

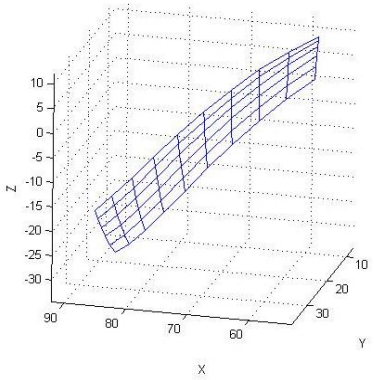

(b) convex surface of pinion

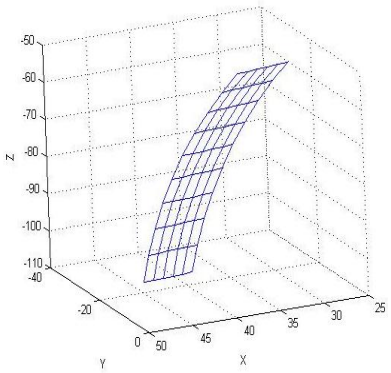

(c) concave of large gear

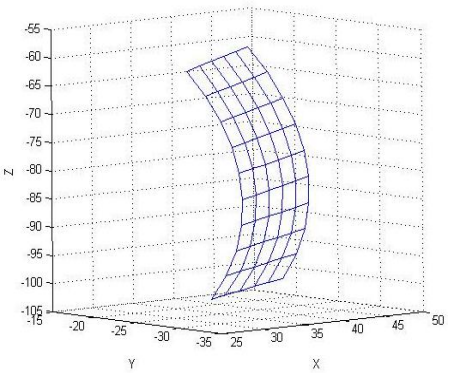

(d) convex surface of large gear

Fig. 13 Tooth surface

C. 3D Geometry Modeling

The data points obtained are introduced into 3D software Pro/E; points, lines, areas and volumes successively

DOI: 10.5963/IJEE0503003

compose a 3D geometry model. A single tooth is shown in Fig. 14; 3D geometry models of pinion and large gear are formed by means of circumvolved array for a single tooth, shown in Figs. 15 and 16.

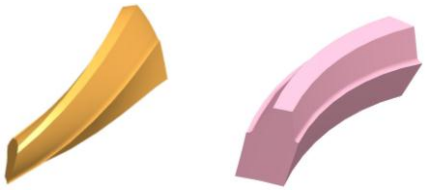

(a) Pinion tooth (b) Large gear tooth

Fig. 14 Teeth comparison

Fig. 15 Geometry model of pinion

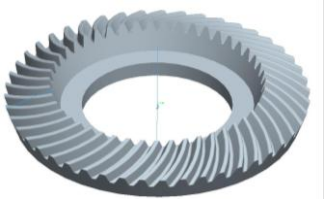

Fig. 16 Geometry model of large gear

VI. ANALYSES OF MESHING CHARACTERISTIC OF EPICYCLOID HYPOID GEAR

A. Multi-body Dynamic Model of Epicycloid Hypoid Gear

The assembled solid model in PROE software was introduced into ADAMS software by means of a public file; then, a rotational motion pair was applied to the gear shaft. The tooth number of large gear and pinion are 47 and 11, respectively. Based on impact function, a solid collision contact model was designed for the contact state between tooth surfaces during meshing; the contact parameters are shown in Table 1. Finally, the virtual prototype model of epicycloid hypoid gear was obtained, as shown in Fig. 17.

TABLE 1 CONTACT PARAMETERS

Name	Content	Name	Content
stiffness coefficient	3.16×10^{9}	static friction coefficient	0.08
drag coefficient	5×10^{4}	dynamic friction coefficient	0.05
force index	1.5	static sliding velocity	0.0001
penetration depth	0.0001	dynamic sliding velocity	0.01

DOI: 10.5963/IJEE0503003

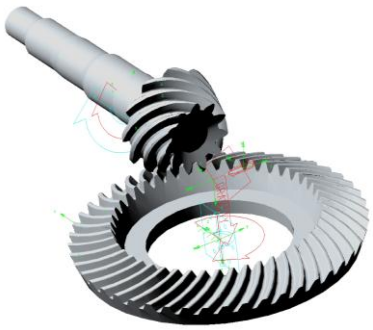

Fig. 17 Multi-body dynamic model of epicycloid hypoid gear

B. Transmission Error Analysis

Loads and constraints shown in Table 1 were applied to a multi-body dynamic system, and the local angular velocity of the transmission error was obtained when the concave component of the pinion drives the convex surface of the large gear, as shown in Fig. 17. The large gear is the follower, and its theoretic angular velocity is 24.4965rad/s. Its change with time for large gear is shown in Fig. 18. The entire oscillogram fluctuates near the root mean square value of 24.5043rad/s. The maximum, minimum and fluctuation amplitude are 25.8962 rad/s, 22.9277 rad/s and 2.9685 rad/s, respectively The root mean square value was compared with the theoretical value; results indicated that transmission error, relative error and fluctuation amplitude error are 0.0078 rad/s, 0.031% and 12.118%, respectively.

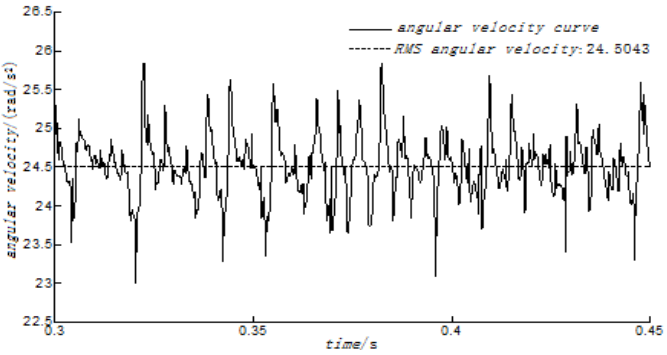

Fig. 18 Change of angular velocity over time for large gear when concave of pinion driving convex surface of large gear

VII. CONCLUSIONS

According to the processing method and cutting tooth processing principle of epicycloid hypoid gear, tool structure, along with relative location and the motion relation between the machine tool and the work piece, a cutting tooth meshing coordinate system developed. Based on cutting tooth meshing principle and space meshing theory, the theoretical tooth face was derived by means of a matrix method. Nonlinear equations were established by discriminating data regarding the theoretical tooth surface. The tooth surface equation was solved by MATLAB software, and discrete data of the tooth surface was obtained. The discrete data was then introduced into Pro/E software, providing a relatively accurate 3D model which provides a model foundation for the succeeding finite element contact analysis, dynamic meshing simulation, etc.

With a practical example, a dynamic simulation of the epicycloid hypoid gear drive system was presented in ADAMS, and the transmission error of epicycloid hypoid gear was obtained when the concave pinion drives the convex surface of the large gear. The angular velocity of follower gear is near its theoretic value, with an error in the allowable range. The model also demonstrates a transmission error of less than 0.2%, indicating a better transmission performance, and in accordance with the actual situation of selecting driving gear for the pinion, finally verifying the accuracy of the 3D model.

ACKNOWLEDGEMENT

It is a Project supported by National Natural Science Foundation of China (Grant No: 51375159); Project supported by The natural science foundation of Hunan Province (Grant No: 2015JJ5020); Project supported by Scientific Research in College Project of Hunan Province, (Grant No: 12A038;13C379).

DOI: 10.5963/IJEE0503003

REFERENCES

[1] TANG Jin-yuan, HUANG Yun-fei, Zhou Chao, et al., "Geometry modelling of spiral bevel gears based on generating tooth-surface," *Computer Simulation*, vol. 26, iss. 2, pp. 293-297, 2009

[2] Chen Shuhan, Yan Hongzhi, Ming Xingzu, et al., "Spiral bevel gears numerical control machining model with six axes five linkages," *Transactions of The Chinese Society for Agricultural Machinery*, vol. 39, no. 10, pp. 198-201, 2008.

[3] Tang Jinyuan, Pu Taiping, and Dai Jin, "Accurate modelling method of a sgm-manufactured spiral bevel gear," *Journal of Mechanical Transmission*, vol. 32, no. 1, pp. 43-46, 2008.

[4] DANG Yu-gong, DENG Xiao-zhong, NIE Shao-wu, et al., "New Scheme of Cold Rotary Forging for Hypoid Gear and Its Feasibility," *Journal Of Beijing University of Technology*, vol. 39, no. 9, pp. 1290-1296, 2013.

[5] Chen Shu-han, Yan Hong-zhi, Ming Xing-zu, et al., "Establishment and analysis of error and difference surfaces in spiral bevel gear," *China Mechanical Engineering*, vol. 19, no. 18, pp. 2156-2161, 2008

[6] Nie Shaowu, Deng Xiaozhong, and Li Tianxing, "Theoretical tooth surface deduction and simulation of orion hypoid gears," *Journal Of Mechanical Transmission*, vol. 33, no. 2, pp. 20-22, 2009.

[7] Chen Shuhan, Yan Hongzhi, Ming Xingzu, et al., "Error modelling and analysis of spiral bevel gear grinder with six axes five linkages," *China Mechanical Engineering*, vol. 19, no. 3, pp. 288-294, 2008.

[8] Deng Jing, Deng Xiaozhong, Xie Junjun, et al., "Study on the structural innovation and gear cutting experiment of hypoid gear for a cnc milling machine tool," *Journal of Mechanical Transmission*, vol. 39, no. 3, pp. 1-4, 2015.

[9] Kil-Young Ahn and Bong-Jo Ryu, "A modeling of impact dynamics and its application to impact force predication," Proceedings of ACMD, vol. 3, no. 2, pp. 448-453, 2004.

[10] Galina I. Sheveleva, Andrey E. Volkov, and Vladimir I. Medvedev, "Algorithms for analysis of meshing and contact of spiral bevel gears," *Source: Mechanism and Machine Theory*, vol. 42, no. 2, pp. 198-215, February 2007.

[11] Faydor L. Litvin, Alfonso Fuentes, and Kenichi Hayasaka, "Design, manufacture, stress analysis, and experimental tests of low-noise high endurance spiral bevel gears," *Source: Mechanism and Machine Theory*, vol. 41, no. 1, pp. 83-118, January 2006.

[12] LI Lin and FENG Meijun, "NC Machining of Spiral Bevel Gear and Hypoid Gear based on Unity Transformation Model," *New Technology & New Process*, no. 2, pp. 52-56, 2014

[13] CHEN Shu-han, YAN Hong-zhi, and MING Xing-zu, "Error modeling and analysis of spiral bevel gear grinder based on multi-body system theory," *Journal of Central South University of Technology*, vol. 15, no. 5, pp. 706-711, 2008.

DOI: 10.5963/IJEE0503003